10

Face Discrimination Using the Orientation and Size Recognition Characteristics of the Spreading Associative Neural Network

Kiyomi Nakamura and Hironobu Takano
Toyama Prefectural University
Japan

1. Introduction

With the rapid progress of the information society, biometrics identification technology has been developed for security applications. Biometrics is person authentication using physical features such as the face, fingerprints, irises, etc. It is advantageous for psychological resistance to be minimized; verification using the face is uninvasive compared with fingerprints. Such security systems using remote monitoring are in demand in customs house and airports, etc.

Recently, face recognition by the on-line processing of facial images has been widely applied in various fields and evaluated the face recognition performance using large scale database (Phillips et al., 2007). The representative face recognition method is classified into two categories. The first is a feature-based approach which uses feature vectors created with complex Gabor wavelet coefficients at each node (Wiskott et al., 1997). The second is the holistic or pattern (template) matching approach. The well-known example for the latter is the approach using eigenfaces which are obtained from principal component analysis of a large number of either full face images (Turk & Pentland, 1991) or local feature images of the face, e.g. eyebrow, eye, nose, cheek, mouth, etc (Penev & Atick, 1996). In both approaches, the conventional nearest neighbor algorithm or neural network is used for face classification.

In personal authentication using facial images, it is a common problem to realize robust recognition independent of variations of illumination, orientation, size, pose, and expression, etc. The various methods of orientation recognition for facial image were proposed (Wong et al., 2001; Wu et al., 2006; Su, 2000). The orientation of facial image obtained by these methods is used for the orientation correction before the face (shape) recognition process. On the other hand, the face size is usually normalized by using the information of distance between eyes or face width. Recently, a rotation and size spreading associative neural network (RS-SAN net) was developed based on space and 3-D shape recognition systems in the brain (Nakamura & Miyamoto, 2001). Using RS-SAN net, a personal authentication method, which was not influenced by the orientation and size changes was proposed. The RS-SAN net correctly recognized face shape, orientation and size, regardless of the input orientation and size, once facial images were learned (Nakamura & Miyamoto, 2001; Nakamura & Takano, 2006). However, the face shape recognition performance of the RS-SAN net was slightly low compared with other face recognition methods.

In this chapter, we introduce a novel face recognition method using the characteristics of orientation and size recognition for decreasing false acceptance. Section 2 and 3 describe the outline of the rotation and size spreading associative neural network (RS-SAN net).

Recognition performances of the orientation, size and shape of faces are evaluated in Section 4. Section 5 details the novel face recognition method which introduces the unlearned face rejection with the orientation and size recognition characteristics. Section 6 concludes this chapter.

2. Rotation and size spreading associative neural network

2.1 Structure of the RS-SAN net

The RS-SAN net consists of orientation, size and shape recognition systems shown in Fig.1. The learning and recognition processes of the RS-SAN net are as follows.

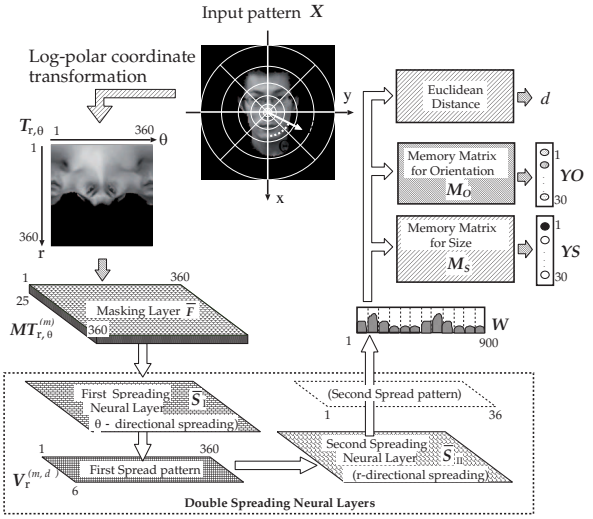

Fig. 1. Structure of the RS-SAN net.

1. The input face pattern $\boldsymbol{X}$ (480 $\times$ 480 pixels) is transformed into a transformed pattern $T_{r,\theta}$ (360 $\times$ 360 pixels) on log-polar coordinates.
2. The transformed pattern is passed through 25 masking layers to produce masked patterns.
3. The double spreading layers spread the 25 masked patterns by weighted orientation and size spreading functions to produce the double spread pattern (900 dimensions).
4. In learning, an orientation memory matrix $\boldsymbol{\mathcal{M}}_{\mathrm{O}}$ and size memory matrix $\boldsymbol{\mathcal{M}}_{\mathrm{S}}$ are obtained from the spread patterns $\boldsymbol{W}_{\mathrm{L}}^{(P)}$ calculated from learning patterns $\boldsymbol{X}^{(P)}$ ($P = 1, \cdots, P_{max}$) and orientation teaching signals $\boldsymbol{TO}^{(P)}$ and size teaching signals $\boldsymbol{TS}^{(P)}$, respectively. The learning was performed in 6 orientations ($0^\circ \sim 300^\circ$ in increments of 60°) $\times$ 6 sizes (same interval in logarithmic scale:1.00, 1.43, 2.04, 2.93, 4.19, 6.00) for respective faces. The spread pattern $\boldsymbol{W}_{\mathrm{L}}^{(P)}$ is also stored in face recognition system for shape recognition.
5. In recognition, the system recognizes the orientation and size at the same time by using the population vectors calculated from the outputs of 30 orientation and size recognition neurons (Georgopoulus et al., 1982). The outputs of orientation and size reecognition neurons are obtained by multiplying the spread patterns $\boldsymbol{W}_{\mathrm{R}}$ calculated from the input pattern $\boldsymbol{X}$ and orientation memory matrix $\boldsymbol{\mathcal{M}}_{\mathrm{O}}$ and size memory matrix $\boldsymbol{\mathcal{M}}_{\mathrm{S}}$, respectively.

The shape is discriminated by the Euclidean distance between the double spread patterns obtained in learning and recognition processes.

2.2 Feature vector calculation

The input face pattern $\boldsymbol{X}$ (480 × 480 pixels) is converted to a transformed pattern $T_{r,\theta}$ (360 × 360 pixels) on the log-polar coordinate system by Eq.(1).

$$T_{r,\theta} = \sum_{i=1}^{3}\sum_{j=1}^{3} I_{x_{ij},y_{ij}} \tag{1}$$

$$(x_{ij} = R\cos\Theta,\ y_{ij} = R\sin\Theta)$$

$$\begin{cases} R = 10^{LI\cdot r} + \left(10^{LI\cdot r} - 10^{LI(r-1)}\right) \times \frac{i}{3} \\ \Theta = (\theta - 1) + \frac{j}{3} \end{cases}$$

$$r,\ \theta = 1, 2, \cdots, 360,\ \ LI = \frac{\log(SR)}{360}$$

where $I_{x_{ij},y_{ij}}$ is the pixel value of the input facial image $\boldsymbol{X}$ at (x_{ij}, y_{ij}) on the Cartesian coordinates and $SR = 240$ is the sampling radius on the input facial image.

The transformed pattern $T_{r,\theta}$ is passed through 25 masking layers to produce 25 masked patterns $MT_{r,\theta}^{(m)}$, $(m = 1, 2, \cdots, 25)$. The masking layers are various spatial filters to extract characteristic features from the transformed image. The various masks $M^{(m)}$ are called spatial filters, and the masked images generated, $MT_{r,\theta}^{(m)}$, are shown in Fig.2. Here, m is a mask number $(m = 1, 2, \cdots, 25)$. A masked image $MT_{r,\theta}^{(m)}$ is calculated by the convolution of the transformed image $T_{r,\theta}$ and a mask $M^{(m)}$. If any pixel value of the masked image is negative $(MT_{r,\theta}^{(m)} < 0)$, the value is set to 0. The masks used in this study extract the edge components of the transformed image. For example, mask $M^{(2)}$ extracts the vertical edge component of a transformed image. The structure of the double spreading layers is shown in Fig.3. The orientation spreading weight $GO_{\theta}^{(d_\theta)}$ $(d_\theta = 1, 2, \cdots, 6)$ in the θ direction has a functional value like that of the Gaussian curve in Eq.(2), and is maximum (1.0) in orientation d_θ as shown in Eq.(3). Similarly, the size spreading weight $GS_{r}^{(d_r)}$ $(d_r = 1, 2, \cdots, 6)$ in the r direction has a functional value like that of the Gaussian curve that is maximum (1.0) in direction d_r as shown in Eqs.(4) and (5). The extent of spreading of the orientation and size information are decided by the spreading coefficients β_θ, β_r in Eqs.(2) and (4), becoming small when these spreading coefficients become larger.

$$F_{S\theta}(x) = \exp\{-\beta_\theta(x - 360n)^2\} \tag{2}$$

$$(-180 + 360n < x \leq 180 + 360n, n = 0, \pm 1, \ldots)$$

$$GO_{\theta}^{(d_\theta)} = F_{S\theta}\{60(d_\theta - 1) - (\theta - 1)\} \tag{3}$$

$$(d_\theta = 1, 2, \cdots, 6\ ,\ \theta = 1, 2, \cdots, 360)$$

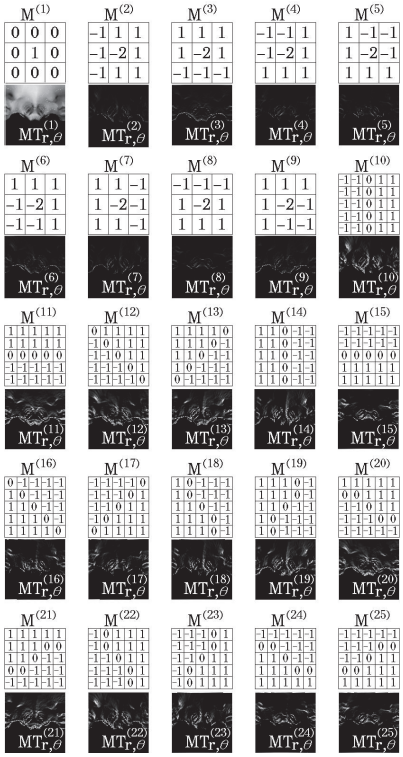

Fig. 2. Masks $M^{(m)}$ and masked images $MT_{r,\theta}^{(m)}$.

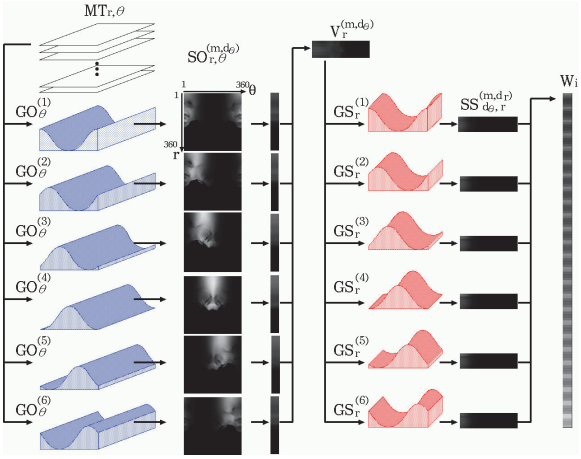

Fig. 3. Structure of the double spreading layers.

$$F_{Sr}(x) = \exp\{-\beta_r(x - 360n)^2\} \quad (4)$$
$$(-180 + 360n < x \leq 180 + 360n, n = 0, \pm 1, \ldots)$$
$$GS_r^{(d_r)} = F_{Sr}\{60(d_r - 1) - (r - 1)\} \quad (5)$$
$$(d_r = 1, 2, \cdots, 6\ ,\ r = 1, 2, \cdots, 360)$$

We obtain the spread image $SO_{r,\theta}^{(m,d_\theta)}$ in the θ direction by multiplying the masked image $MT_{r,\theta}^{(m)}$ and $GO_\theta^{(d_\theta)}$ in Eq.(6), and the spread vector $V_r^{(m,d_\theta)}$ by the summation of $SO_{r,\theta}^{(m,d_\theta)}$ concerning θ by Eq.(7). Then, we obtain the spread image $SS_{d_\theta,r}^{(m,d_r)}$ in the r direction by multiplying $V_r^{(m,d_\theta)}$ and $GS_r^{(d_r)}$ in Eq.(8). Finally, the double spread vector $\boldsymbol{W}^{*(P)}$ is obtained by summation of $SS_{d_\theta,r}^{(m,d_r)}$ concerning r by Eq.(9). The dimension of $\boldsymbol{W}^{*(P)}$ is decided by d_r, d_θ and m. This reaches 900 dimensions by multiplying $6(d_\theta) \times 6(d_r) \times 25(m)$ in Eq.(10).

$$SO_{r,\theta}^{(m,d_\theta)} = MT_{r,\theta}^{(m)} \times GO_\theta^{(d_\theta)} \quad (6)$$
$$V_r^{(m,d_\theta)} = \sum_{\theta=1}^{360} SO_{r,\theta}^{(m,d_\theta)} \quad (7)$$
$$SS_{d_\theta,r}^{(m,d_r)} = V_r^{(m,d_\theta)} \times GS_r^{(d_r)} \quad (8)$$
$$W_i^* = \sum_{r=1}^{360} SS_{d_\theta,r}^{(m,d_r)} \quad (9)$$
$$(i = 36 \cdot (m - 1) + 6 \cdot (d_\theta - 1) + d_r)$$
$$\boldsymbol{W}^{*(P)} = [W_1^*, \cdots, W_{900}^*]^T \quad (10)$$

To remove the bias of $\boldsymbol{W}^*$ which degrades the recognition performance, the normalized double spread vector $\boldsymbol{W}$ is obtained by Eqs.(11) and (12). As a feature vector of the face pattern $\boldsymbol{X}$, the normalized double spread pattern $\boldsymbol{W}$ is used for both learning (registration) and recollection (recognition).

$$||\boldsymbol{W}^*|| = \sqrt{\sum_{i=1}^{900} W_i^{*2}} \quad (11)$$
$$\boldsymbol{W} = \frac{\boldsymbol{W}^*}{||\boldsymbol{W}^*||} \quad (12)$$

2.3 Recognition neuron

2.3.1 Orientation recognition neuron

The orientation angle of a facial image is indicated by the orientation of a population vector ϕ_o. The ϕ_o is defined as an ensemble of vectors of the orientation recognition neurons $\boldsymbol{YO} = [YO_1, \cdots, YO_{30}]^T$ where each vector points to the neuron's optimally tuned orientation and has a length in proportion to the neuron's output (Georgopoulus et al., 1982). The arrangement of orientation neurons and the orientation population vector are shown in Fig.4. This assumes that the neurons in the parietal cortex (PG) of the brain recognize the axis orientation of an object by population coding, as seen in neurophysiological studies. Each orientation recognition neuron YO_i has a respective representative orientation ψ_i that characterizes the best orientation for the optimal response in Eq.(13). The population

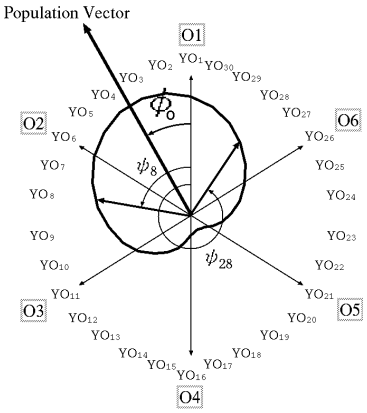

Fig. 4. Arrangement of orientation recognition neurons and population vector.

vector orientation ϕ_o is calculated by the vectorial summation of 30 orientation neurons $(YO_1, \cdots, YO_{30})$ by Eq.(14).

$$\psi_i = \frac{2\pi}{30} \times (i-1) \qquad (i = 1, 2, \cdots, 30) \tag{13}$$

$$\phi_o = \tan^{-1}\left(\sum_{i=1}^{30} YO_i \sin\psi_i \Big/ \sum_{i=1}^{30} YO_i \cos\psi_i\right) \tag{14}$$

2.3.2 Size recognition neuron

The size of a facial image is also indicated as a direction of a population vector ϕ_S. The arrangement of size recognition neurons and size population vector are shown in Fig.5. This assumes that the neurons in the PG of the brain recognize the size of an object by population coding. Each size recognition neuron has a respective representative size that characterizes the best size for the optimal response. For example, the size neuron YS_{10} has a optimal response for the size of the facial image $S4$ (2.93) and the neurons around YS_{10} also have moderate responses to the same size. The population vector size ϕ_S is calculated by the vectorial summation of 30 size recognition neurons $(YS_1, \cdots, YS_{30})$ by Eq.(15). Between sizes $S1$ and $S6$, there are undefined size ranges, because the sizes $S1$ to $S6$ are not continuous. If the size population vector indicates an undefined range, the size of the facial image will not be obtained in Eq.(16).

$$\phi_s = \tan^{-1}\left(\sum_{i=1}^{30} YS_i \sin\psi_i \Big/ \sum_{i=1}^{30} YS_i \cos\psi_i\right) \tag{15}$$

$$\eta = \begin{cases} 10^{\frac{\log 6}{\pi}\cdot\phi_s} & (-\frac{\pi}{5} \le \phi_s \le \frac{6}{5}\pi) \\ undefine & (-\frac{4}{5}\pi \le \phi_s \le -\frac{\pi}{5}) \end{cases} \tag{16}$$

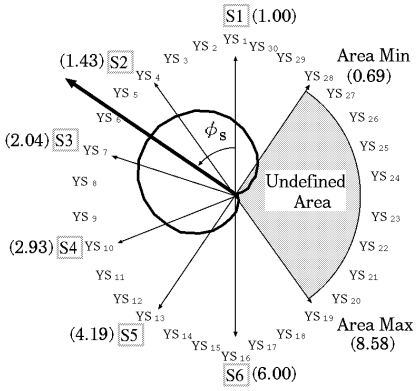

Fig. 5. Arrangement of size recognition neurons and population vector.

3. Learning (registration) and recognition

In the learning process of orientation and size, the RS-SAN net uses generalized inverse learning (Nakano, 1990; Amari, 1978), developed in 6 orientations ($0° \sim 300°$ in increments of $60°$) $\times$ 6 sizes (same interval in logarithmic scale:1.00, 1.43, 2.04, 2.93, 4.19, 6.00) for respective faces. In the typical case of learning 10 human faces, the 360 patterns (=10 faces $\times$ 6 orientations $\times$ 6 sizes) normalized double spread patterns $\boldsymbol{W}_{\mathrm{L}}^{(P)}$ ($P = 1, \cdots, 360$) are memorized. In the learning process of the face shape, the specified normalized double spread patterns $\boldsymbol{W}_{\mathrm{L}}^{(P)}$ corresponding to specified orientation and size (typically, orientation = $0°$ and size = 6.0) of the respective faces are registered.

3.1 Teaching signal

3.1.1 Orientation recognition neuron

The teaching signal for orientation recognition $\boldsymbol{TO}^{(P)}$ is shown in Fig.6. There were six training signals $\boldsymbol{KO}^{(d_o)}$ corresponding to the six orientations d_o to be memorized. The desired outputs of the orientation recognition neurons were broadly tuned to the orientation of the facial image and adjusted to the function in Eq.(17). The desired outputs of orientation

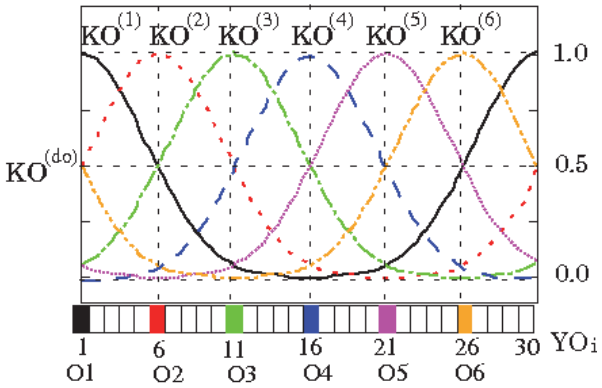

Fig. 6. Teaching signal for orientation recognition.

recognition neurons $\boldsymbol{TO}^{(P)}$ in Eq.(20) are fitted to $\boldsymbol{KO}^{(d_o)}$ which is the Gaussian curve function defined by Eqs.(17) and (18). For example, when the RS-SAN net memorizes orientation $O4(180^\circ)$, the maximum value of the Gaussian curve function in Eq.(17) fits the orientation recognition neuron YO_{16}. This training signal is the same irrespective of the size and shape of the facial image when the orientation of other learned facial image is the same.

$$F_{TO}(x) = \exp\left\{-\alpha_o(x-30n)^2\right\} \tag{17}$$
$$(-15+30n < \ x \ \leq 15+30n, n=0,\pm1,\ldots)$$
$$KO_i^{(d_o)} = F_{TO}\left\{5(d_o-1)-(i-1)\right\} \tag{18}$$
$$(d_o = 1,2,\cdots,6\ ,\ i=1,2,\cdots,30)$$
$$\boldsymbol{KO}^{(d_o)} = [KO_1^{(d_o)}, KO_2^{(d_o)}, \cdots, KO_{30}^{(d_o)}]^T \tag{19}$$
$$\boldsymbol{TO}^{(P)} = \boldsymbol{KO}^{(d_o)} \tag{20}$$

Here, $P\ (=\ 1,\cdots,360)$ is the training pattern number, $d_o\ (=\ 1,\cdots,6)$ is the training orientation of the P-th training pattern, $i\ (=\ 1,\cdots,30)$ is the number of the orientation recognition neuron, and α_o is the coefficient that defines the tuning width of the teaching signal for orientation recognition neurons.

3.1.2 Size recognition neuron

The teaching signal for orientation recognition $\boldsymbol{TS}^{(P)}$ is shown in Fig.7. There were six size training signals $\boldsymbol{KS}^{(d_s)}$ corresponding to the six sizes d_s to be memorized. The desired outputs of the size memory neurons were broadly tuned to the size of the facial image and adjusted to the function in Eq.(21). The desired outputs of the size recognition neurons $\boldsymbol{TS}^{(P)}$ in Eq.(24) were fitted to $\boldsymbol{KS}^{(d_s)}$, which is the Gaussian curve function defined by Eqs.(21) and (22). For example, when RS-SAN net memorizes size $S2$ (1.43), the maximum value of the Gaussian curve function in Eq.(21) fits the size memory neuron YS_4. This training signal is the same irrespective of the orientation and shape of the facial image when the size of other learned facial image is the same.

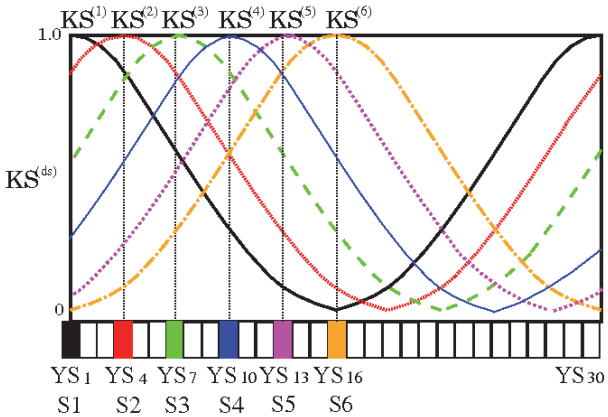

Fig. 7. Teaching signal for size recognition.

$$F_{TS}(x) = \exp\left\{-\alpha_s(x-30n)^2\right\} \tag{21}$$
$$(-15+30n < \ x \ \leq 15+30n, n=0,\pm1,\ldots)$$
$$KS_j^{(d_s)} = F_{TS}\left\{3(d_s-1)-(j-1)\right\} \tag{22}$$
$$(d_s = 1,2,\cdots,6\ ,\ j=1,2,\cdots,30)$$
$$\boldsymbol{KS}^{(d_s)} = [KS_1^{(d_s)}, KS_2^{(d_s)}, \cdots, KS_{30}^{(d_s)}]^T \tag{23}$$
$$\boldsymbol{TS}^{(P)} = \boldsymbol{KS}^{(d_s)} \tag{24}$$

Here, $P\ (=1\sim360)$ is the training pattern number, $d_s\ (=1\sim6)$ is the learning size number of the P-th training pattern, j is the size memory neuron number, and α_s is the coefficient that decides the tuning width of teaching signal for size recognition neurons in Eq.(21).

3.2 Learning (registration) process

The RS-SAN net uses generalized inverse learning for orientation and size recognition. The double spread pattern $\boldsymbol{W}_{\mathrm{L}}^{(P)}$ is obtained from the P-th training input pattern in the double spreading layers. The orientation memory matrix $\boldsymbol{\mathcal{M}}_{\mathrm{O}}$ is obtained by associating $\boldsymbol{W}_{\mathrm{L}}^{(P)}$ with the desired outputs of orientation recognition neurons $\boldsymbol{TO}^{(P)}$ by Eq.(27). The size memory matrix $\boldsymbol{\mathcal{M}}_{\mathrm{S}}$ is obtained by associating $\boldsymbol{W}_{\mathrm{L}}^{(P)}$ with the desired outputs of size recognition neurons $\boldsymbol{TS}^{(P)}$ $(P=1,\cdots,360)$ by Eq.(28). For the shape learning of the faces, the double spread patterns $\boldsymbol{W}_{\mathrm{L}}^{(P)}$ of specified orientation (= 0°) and size (= 6.0) for the respective faces are registered in the face recognition system.

$$\boldsymbol{\mathcal{X}} = [\boldsymbol{W}_{\mathrm{L}}^{(1)}, \boldsymbol{W}_{\mathrm{L}}^{(2)}, \cdots, \boldsymbol{W}_{\mathrm{L}}^{(360)}] \tag{25}$$
$$\boldsymbol{\mathcal{X}}^{+} = (\boldsymbol{\mathcal{X}}^T\boldsymbol{\mathcal{X}})^{-1}\boldsymbol{\mathcal{X}}^T \tag{26}$$
$$\boldsymbol{\mathcal{M}}_{\mathrm{O}} = \boldsymbol{\mathcal{TO}}\boldsymbol{\mathcal{X}}^{+} \tag{27}$$
$$\boldsymbol{\mathcal{TO}} = [\boldsymbol{TO}^{(1)}, \boldsymbol{TO}^{(2)}, \cdots, \boldsymbol{TO}^{(360)}]$$
$$\boldsymbol{\mathcal{M}}_{\mathrm{S}} = \boldsymbol{\mathcal{TS}}\boldsymbol{\mathcal{X}}^{+} \tag{28}$$
$$\boldsymbol{\mathcal{TS}} = [\boldsymbol{TS}^{(1)}, \boldsymbol{TS}^{(2)}, \cdots, \boldsymbol{TS}^{(360)}]$$

3.3 Recognition process

In the recognition process, the system simultaneously recognizes the orientation and size of the facial image. First, the double spread pattern $\boldsymbol{W}_{\mathrm{R}}$ used for recognition is generated with the input facial image. For face orientation recognition, the orientation memory matrix $\boldsymbol{\mathcal{M}}_{\mathrm{O}}$ is multiplied by $\boldsymbol{W}_{\mathrm{R}}$ in Eq.(29), and the output of orientation recognition neurons $\boldsymbol{YO}$ is obtained. For face size recognition, the size memory matrix $\boldsymbol{\mathcal{M}}_{\mathrm{S}}$ is multiplied by $\boldsymbol{W}_{\mathrm{R}}$ in Eq.(30), and the output of size recognition neurons $\boldsymbol{YS}$ is obtained.

$$\boldsymbol{YO} = \boldsymbol{\mathcal{M}}_{\mathrm{O}}\boldsymbol{W}_{\mathrm{R}} \tag{29}$$
$$\boldsymbol{YS} = \boldsymbol{\mathcal{M}}_{\mathrm{S}}\boldsymbol{W}_{\mathrm{R}} \tag{30}$$

The orientation is recognized by the population vector calculated from the outputs of 30 orientation recognition neurons. The size is also recognized by the population vector calculated from the outputs of 30 size recognition neurons.

The shape is discriminated by the Euclidean distance between the double spread patterns obtained in learning and recognition processes. The value of Euclidean distance (d) in Eq.(31) has the range of $0 \leq d \leq 2$, because the norm of spread pattern is normalized as 1. When it has the minimum value of "0", resemblance is the highest. The double spread pattern $\boldsymbol{W}'_{\mathrm{R}}$ used for the shape recognition is generated by correcting the orientation and size of the input facial image to the pre-determined specified ones (typically, orientation = 0° and size = 6.0). The orientation and size of the corrected facial image correspond to those of the learned face. The orientation and size correction prevents the deterioration of the shape recognition performance.

$$d = ||\boldsymbol{W}_{\mathrm{L}} - \boldsymbol{W}'_{\mathrm{R}}|| \tag{31}$$

4. Face recognition experiment

The characteristics of orientation, size and shape recognition for learned and unlearned faces were investigated with face database collected at The University of Essex (Spacek, 2008). The 70 facial images of 35 subjects (2 images for each subject) were used for recognition experiments. In preprocessing, the background and clothing areas were excluded. The image size and format were converted to 480×480 [pixels] and gray scaled (256 steps), respectively. The facial images in the learning and recognition tests were at size 6.0 and orientation 0°. For the convenience sake, one facial image obtained from 35 subjects was used for training in 6 x 6 orientations and sizes. The orientation and size recognition tests were examined using 6 facial images (another learned facial image and five unlearned faces). We tried 35 sets of recognition tests by changing the learning and recognition facial images one by one. Recognition results were thus obtained for 210 trials consisting of 35 trials for learned faces and 175 for unlearned faces. In shape recognition test, 10 facial images (another learned facial image and 9 unlearned facial images) among 35 subjects were recollected for each learned face. Thus, 350 recognition trials consisting of 35 trials for learned faces and 315 trials for unlearned faces were examined. The shape recognition was evaluated using the false rejection rate (FRR) and false acceptance rate (FAR). When the output of Euclidean distance calculated for learned face is higher than the decision threshold, we considered that the registered face was erroneously rejected and calculated the false rejection rate by counting the trials of false rejection. On the other hand, when the output of Euclidean distance calculated for unlearned face was lower than the decision threshold, we considered that the imposters were accepted incorrectly. We calculated the false acceptance rate by counting the trials of false acceptance.

4.1 Orientation recognition performance

The orientation recognition result for learned and unlearned faces was shown in Fig.8. The horizontal axis is the input face number, and the vertical axis is the recognized orientation angle. The average $\pm$ standard deviation of recognized orientation for learned and unlearned faces were $0.47 \pm 1.89[^\circ]$ and $3.74 \pm 43.69[^\circ]$, respectively. As shown in Fig.8, the recognized orientation of learned faces distributed around 0 degree; however, the recognized orientation of unlearned faces was heavily dispersed (SD was very large). The histogram of absolute error of recognized orientation angle for learned and unlearned faces was shown in Fig.9. The horizontal axis is the absolute error of recognized orientation angle, and the vertical axis is the percentage of facial image included in each bin. The white and black bars show the distribution of the absolute error of recognized orientation for learned and unlearned faces, respectively. The absolute error of recognized orientation for learned faces was less than 4 degrees; however, the absolute error of recognized orientation for most of unlearned faces distributed more than 5 degrees.

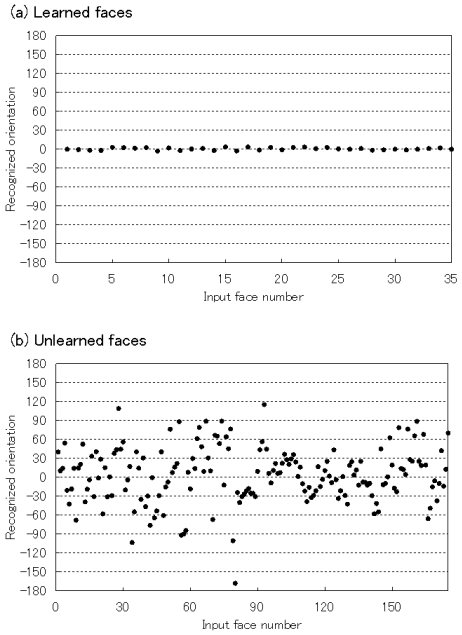

Fig. 8. Orientation recognition result for (a) learned and (b) unlearned faces.

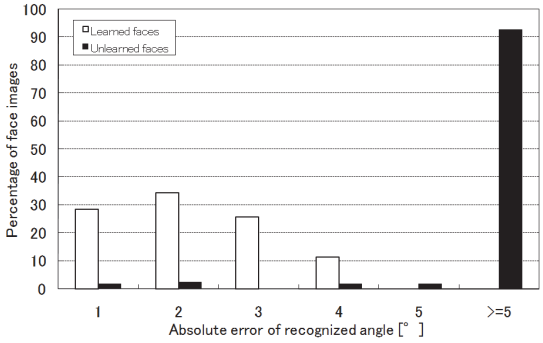

Fig. 9. Histogram of absolute error of recognized orientations for learned and unlearned faces.

4.2 Size recognition performance

The size recognition result for learned and unlearned faces was shown in Fig.10. The horizontal axis is the input face number, and the vertical axis is the recognized size. The average ± standard deviation of recognized size for learned and unlearned faces were 6.03 ± 0.26 and 5.51 ± 2.78, respectively. As shown in Fig.10, the recognized size of learned faces distributed around 6, which means the registered face size; however, the recognized size of unlearned faces was heavily dispersed (SD was very large). The histogram of absolute error of recognized size for learned and unlearned faces was shown in Fig.11. The horizontal

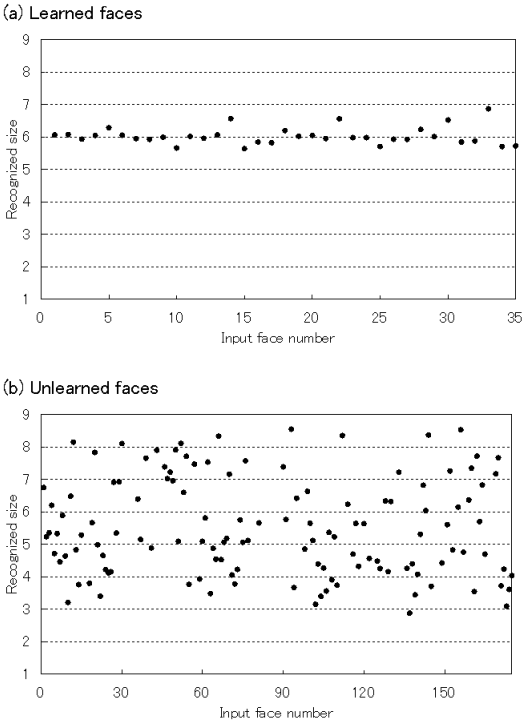

Fig. 10. Size recognition result for (a) learned and (b) unlearned faces.

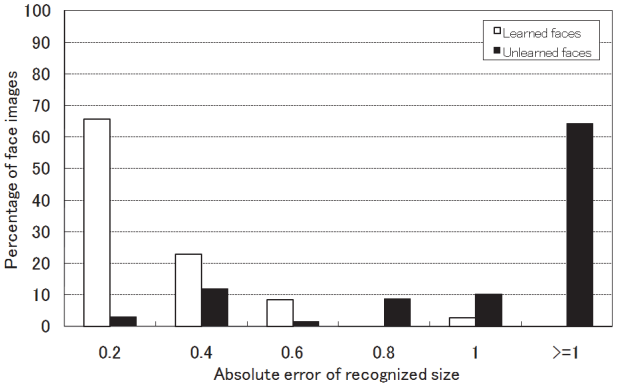

Fig. 11. Histogram of absolute error of recognized size for learned and unlearned faces.

axis is the absolute error of recognized size, and the vertical axis is the percentage of facial image included in each bin. The white and black bars show the distribution of the absolute error of recognized size for learned and unlearned faces, respectively. The absolute error of

recognized size for learned faces was less than 1; however, 64 % absolute error of recognized size for unlearned faces distributed more than 1.

4.3 Shape recognition performance

Shape recognition performance was evaluated using equal error rate (EER) determined by finding the point where false acceptance rate intersects the false rejection rate. The result of shape recognition is shown in Fig.12. The horizontal axis is the decision threshold for discriminating between registered faces and imposters. The vertical axis is the FRR and FAR. Circle and solid line show the FAR. Square and dashed line show the FRR. The equal error rate was 2.86 % when the decision threshold of Euclidean distance was 0.13. At and below the decision threshold criterion of 0.06, the FAR was 0 %, even if the FRR was 34 %.

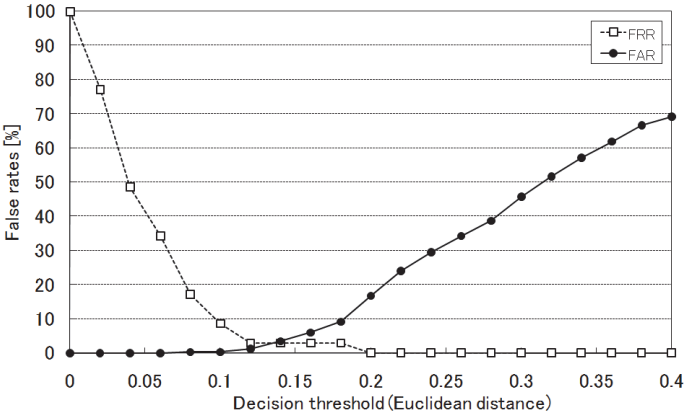

Fig. 12. False acceptance and rejection rates obtained with Euclidean distance.

5. Unlearned face rejection with recognized orientation and size

The orientation and size recognition performances indicated the RS-SAN net had fairly good orientation and size recognition characteristics for learned faces. On the other hand, the orientation angle and size of unlearned faces were hardly recognized because the distributions of recognized orientation angle and size were widely dispersive. Thus, the RS-SAN net can recognize simultaneously both orientation and size of only learned faces. Using the difference of orientation and size recognition characteristics between learned and unlearned faces, the unlearned face would be removed before face discrimination with Euclidean distance. The flowchart of new face (shape) recognition processes is shown in Fig.13. Before shape recognition using Euclidean distance calculated with double spread patterns, the unregistered faces are rejected using the averages and standard deviations of recognized orientation angle (θ_{av}, σ_o) and size (S_{av}, σ_s) for learned faces obtained by the RS-SAN net. The input face is determined as imposter if the recognized orientation is out of $\theta_{av} \pm 3\sigma_o$. If the recognized size is greater than $S_{av} + 3.2\sigma_s$ or less than $S_{av} - 3.2\sigma_s$, the input face is also rejected as imposter. Note that all of learned faces are not rejected with the orientation and size discrimination because the recognized orientation and size for learned faces were within $\theta_{av} \pm 3\sigma_o$ and $S_{av} \pm 3.2\sigma_s$.

The shape recognition performance obtained by new recognition method was shown in Fig.14. The horizontal axis is the decision threshold for discriminating between registered faces and

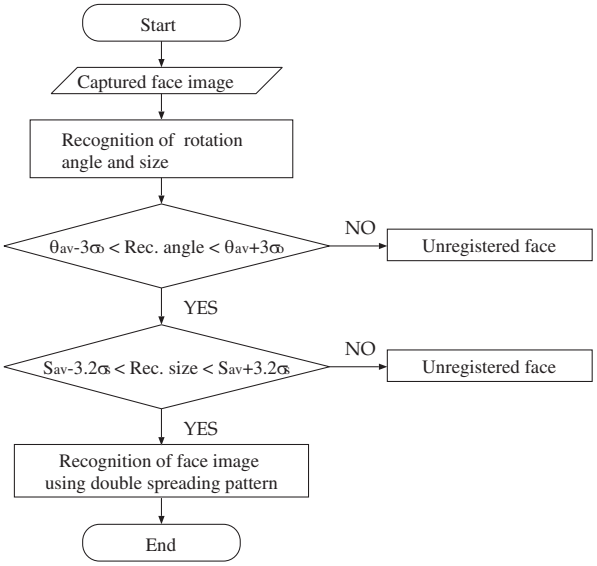

Fig. 13. Flowchart of new shape recognition process using the characteristics of orientation and size recognition.

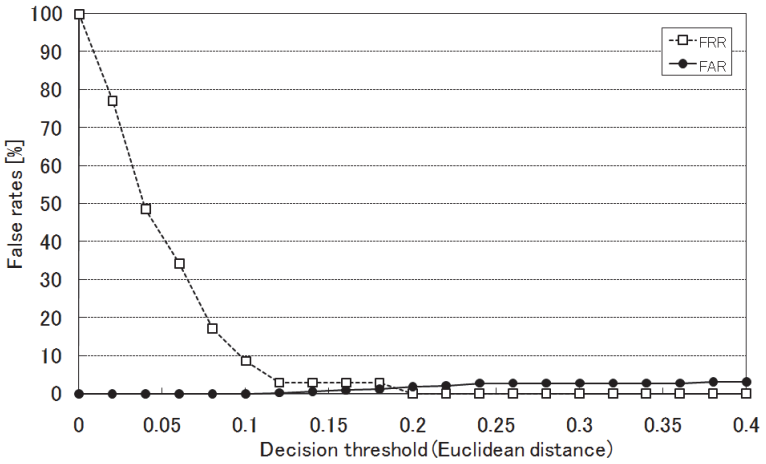

Fig. 14. False acceptance and rejection rates obtained by new face discrimination method with the characteristics of orientation and size recognition.

imposters. The vertical axis is the FRR and FAR. Circle and solid line show the FAR. Square and dashed line show the FRR. The facial images used for learning and recognition are the same as Section 4. This result indicated the FAR drastically decreased. The equal error rate was 1.56 % at the decision threshold of 0.19. When the false acceptance rate was 0 %, the false rejection rate decreased from 34 % to 8.6 %. The criteria of imposter rejection are empirically determined using the experimental results of the orientation and size recognition. To raise

reliability of these decision criteria, the orientation and size recognition characteristics of the learned and unlearned faces would be investigated with large-scale database; however, the experimental result indicates that the unregistered face rejection by the recognized orientation and size is very effective to improve the shape recognition performance.

6. Conclusions

In this chapter, we showed the recognition characteristics of the RS-SAN net for the learned and unlearned faces. The RS-SAN net can recognize both orientation angle and size for learned faces. On the other hand, both orientation and size for unlearned faces were not obtained by the RS-SAN net because the recognized orientation and size were heavily dispersed from the orientation and size of input face. In the shape recognition, the equal error rate was 2.86 % at decision threshold of 0.13.

The RS-SAN net has the unique characteristics of the orientation and size recognition. The orientation and size of only learned face were recognized correctly. However, the recognized orientation and size of unlearned faces were heavily scattered. By introducing the unlearned face discrimination with the recognized orientation and size, new shape recognition method was developed. The experimental result of new shape recognition method showed that the false acceptance rate decreased drastically, even in very high decision threshold. The false acceptance rates were almost constant (about $2 \sim 3$ %) across the decision threshold ranging from 0.2 to 0.4. The imposter rejection method using recognized orientation and size provided the effective improvement of the face recognition performance. The equal error rate decreased to 1.56 % at the decision threshold of 0.19, and the false rejection rate also decreased to 8.6 % at a false acceptance rate of 0 %. Though the scale of the face database used in the present study was small, the face recognition performance in the present study was almost comparable with those reported in FRVT 2006 using large scale database (Phillips et al., 2007). The characteristics of recognition algorithm in the present stuty is that the false acceptance rates can be reduced dramatically even in the condition of very high decision threshold. This characteristics will not be concerned with the scale of the database.

In future studies, we will automatically detect the facial area using skin color information or appearance-based method, e.g. Haar-like features (Viola & Jones, 1996), and correct the facial center using positional information of both eyes. In addition, the recognition experiment will be examined with many more samples of facial images to obtain the decision criteria of the imposter rejection combined with the orientation and size recognition.

7. References

Phillips, P. J.; Scruggs, W. T.; O'Toole, A. J.; Flynn, P. J.; Bowyer, K. W.; Schott, C. L. & Sharpe, M. (2007). FRVT 2006 and ISCE 2006 large-scale results, 15.03.2011, Available from http://www.frvt.org/.

Wiskott, L.; Fellous, J.; Kruger, N. & Malsburg, C. von der (1997). Face recognition by elastic bunch graph matching. *PAMI*, Vol.19, No.7, pp.775-779.

Turk, M. & Pentland, A. (1991). Eigenfaces for recognition. *J. Cognitive Neurosci.*, Vol. 3, No. 1, pp. 71-86.

Penev, P. S. & Atick, J. J. (1996). Local feature analysis: A general statistical theory for object representation. *Neural Systems*, Vol. 7, No. 3, pp. 477-500.

Wong, K.-W.; Lam, K.-M. & Siu, W.-C. (2001). An efficient algorithm for human face detection and facial feature extraction under different conditions. *Pattern Recognition*, Vol. 34, No. 10, pp. 1993-2004.

Wu, S.; Jiang, L.; Xie, S. & Yeo, A. C. B. (2006). A robust method for detecting facial orientation in infrared images. *Pattern Recognition*, Vol. 39, No. 2, pp. 303-309.

Su, C.-L. (2000). Face recognition by using feature orientation and feature geometry matching. *J. Intell. Robotic Syst.*, Vol. 28, No. 1, pp. 159-169.

Nakamura, K. & Miyamoto, S. (2001). Rotation, size and shape recognition by a spreading associative neural network. *IEICE Trans. Inf. & Syst.*, Vol. E-84-D, No. 8, pp. 1075-1084.

Nakamura, K. & Takano, H. (2006). Rotation and size independent face recognition by the spreading associative neural network. *Proc. IEEE World Congress on Comp. Intell. (WCCI2006)*, pp. 8213-8219.

Nakano, K. (1990). *An Introduction to Neurocomputing*, Corona Publishing, Tokyo.

Amari, S. (1978). *A Mathematical Principle of Neural Networks*, Sangyo Publishing, Tokyo.

Georgopoulus, A. P.; Kalaska, J. F.; Caminiti, R. & Massey, J. T. (1982). On the relations between the direction of two-dimensional arm movements and cell discharge in primate motor cortex. *J. Neurosci.*, Vol. 2, No. 11, pp. 1527-1537.

Spacek, L. (2008). Face Recognition Data, 15.03.2011, Available from http://cswww.essex.ac.uk/mv/allfaces/index.html.

Viola, P. & Jones, M. J. (2004). Robust real-time face detection. *Int. J. Computer Vision*, Vol. 57, No. 2, pp. 137-154.

New Approaches to Characterization and Recognition of Faces
Edited by Dr. Peter Corcoran

ISBN 978-953-307-515-0
Hard cover, 252 pages
Publisher InTech
Published online 01, August, 2011
Published in print edition August, 2011

As a baby, one of our earliest stimuli is that of human faces. We rapidly learn to identify, characterize and eventually distinguish those who are near and dear to us. We accept face recognition later as an everyday ability. We realize the complexity of the underlying problem only when we attempt to duplicate this skill in a computer vision system. This book is arranged around a number of clustered themes covering different aspects of face recognition. The first section presents an architecture for face recognition based on Hidden Markov Models; it is followed by an article on coding methods. The next section is devoted to 3D methods of face recognition and is followed by a section covering various aspects and techniques in video. Next short section is devoted to the characterization and detection of features in faces. Finally, you can find an article on the human perception of faces and how different neurological or psychological disorders can affect this.

InTech Europe
University Campus STeP Ri
Slavka Krautzeka 83/A
51000 Rijeka, Croatia
Phone: +385 (51) 770 447
Fax: +385 (51) 686 166
www.intechopen.com

InTech China
Unit 405, Office Block, Hotel Equatorial Shanghai
No.65, Yan An Road (West), Shanghai, 200040, China
中国上海市延安西路65号上海国际贵都大饭店办公楼405单元
Phone: +86-21-62489820
Fax: +86-21-62489821